Antivascular Therapy of Human Follicular Thyroid Cancer Experimental Bone Metastasis by Blockade of Epidermal Growth Factor Receptor and Vascular Growth Factor Receptor Phosphorylation

Maher Nabil Younes,[1] Orhan Gazi Yigitbasi,[1] Young Wook Park,[1] Sun-Jin Kim,[2] Samar A. Jasser,[1] Valerie Stone Hawthorne,[3] Yasemin Dakak Yazici,[1] Mahitosh Mandal,[1] Benjamin Nebiyou Bekele,[4] Corazon D. Bucana,[2] Isaiah J. Fidler,[2] and Jeffrey N. Myers[1,2]

Departments of [1]Head and Neck Surgery, [2]Cancer Biology, [3]Surgical Oncology, and [4]Biostatistics, The University of Texas M.D. Anderson Cancer Center, Houston, Texas

Abstract

Patients suffering from bone metastases of follicular thyroid carcinoma (FTC) have a poor prognosis because of the lack of effective treatment strategies. The overexpression of epidermal growth factor receptor (EGFR) associated with increased vascularity has been implicated in the pathogenesis of FTC and subsequent bone metastases. We hypothesized that inhibiting the phosphorylation of the EGFR and vascular endothelial growth factor receptor (VEGFR) by AEE788, a dual tyrosine kinase inhibitor of EGFR and VEGFR, in combination with paclitaxel would inhibit experimental FTC bone lesions and preserve bone structure. We tested this hypothesis using the human WRO FTC cell line. In culture, AEE788 inhibited the EGF-mediated phosphorylation of EGFR, VEGFR2, mitogen-activated protein kinase, and Akt in culture. AEE788, alone and in combination with paclitaxel, inhibited cell growth and induced apoptosis. When WRO cells were injected into the tibia of nude mice, tumor and endothelial cells within the lesions expressed phosphorylated EGFR, VEGFR, Akt, and mitogen-activated protein kinase that were inhibited by the oral administration of AEE788. Therapy consisting of orally given AEE788 and i.p. injected paclitaxel induced a high level of apoptosis in tumor-associated endothelial cells and tumor cells with the inhibition of tumor growth in the bone and the preservation of bone structure. Collectively, these data show that blocking the phosphorylation of EGFR and VEGFR with AEE788 combined with paclitaxel can significantly inhibit experimental human FTC in the bone of nude mice. (Cancer Res 2005; 65(11): 4716-27)

Introduction

Thyroid cancer is the most common endocrine neoplasm in the United States (1). The incidence of thyroid cancer has been growing at an alarming rate of 3% annually (2). Histologically, 94% of thyroid carcinomas are well differentiated; this group includes papillary thyroid carcinomas and follicular thyroid carcinomas (FTC; ref. 3). Of the well-differentiated thyroid cancers, FTC accounts for 10% to 32% of cases (4, 5).

Requests for reprints: Jeffrey N. Myers, Department of Head and Neck Surgery, The University of Texas M.D. Anderson Cancer Center, Unit 441, 1515 Holcombe Boulevard, Houston, TX 77030-4009. Phone: 713-792-6920; Fax: 713-794-4662; E-mail: jmyers@mdanderson.org.

Although differentiated thyroid cancers are associated with a favorable long-term survival, the prognosis worsens dramatically for patients with distant metastases (6). Whereas the 20-year disease-specific survival rate in patients with differentiated thyroid cancer exceeds 90%, the 10-year survival rate following the detection of bone metastases is <20% (7). Although patients with FTC rank second in survival rates behind those with papillary thyroid cancer, patients with FTC face an increased risk of developing metastases in the lung and bone (8). In fact, metastases from FTC occur earlier and are more aggressive than those from papillary thyroid cancer (5). At diagnosis, bone metastasis is present in ~10% to 30% of patients with FTC (9).

In addition to a decreased survival, patients with bone metastases from FTC have marked morbidity associated with severe pain, pathologic fractures, life-threatening hypercalcemia, and spinal cord compression (10). The current palliative options for bone metastasis include chemotherapy (6), external radiation therapy (11), arterial embolization (12), and radioactive iodine (13), but none of these modalities has thus far been effective in slowing the progression of the disease (14). Surgical management of bone lesions includes the prophylactic stabilization of impending fractures or the fixation of actual fractures with hardware or prosthetic devices (15). However, metastatic follicular cancer is almost invariably multifocal, involving several bones, hence preventing complete surgical resection (16, 17). Clearly, new treatment strategies for patients with FTC bone metastasis are urgently needed.

Among the potential therapeutic targets in the management of FTC bone metastasis is the epidermal growth factor (EGF)/EGF receptor (EGFR) pathway. The EGF and EGFR are overexpressed in thyroid carcinomas in comparison with normal thyroid tissue (18). EGF stimulates the growth, proliferation, and invasion of FTC cells and the blockade of EGFR signaling decreases the growth and invasion of FTC cells *in vitro* (19). In fact, high expression of EGFR is associated with poor prognosis in thyroid tumors (18). The coexpression of EGF and EGFR is also associated with bone metastasis of FTC (20).

Angiogenesis is another important potential therapeutic target for the treatment of FTC-induced bone metastasis. Angiogenesis, the formation of new blood vessels, plays an integral part in the pathogenesis and spread of differentiated thyroid cancer. Actually, FTC is the most angiogenesis-dependent tumor of the thyroid gland (21). One of the major proangiogenic factors in thyroid tumors is vascular endothelial growth factor (VEGF; ref. 22). The level of VEGF mRNA and protein is associated with mitogenic

activity and tumorigenic potential by FTC cell lines (23). The overexpression of VEGF in differentiated thyroid cancer has been correlated with poor prognosis (4, 24), increased risk of recurrence, and greater probability of metastasis (25) as well as increased microvessel density (MVD) with decreased disease-free survival in thyroid carcinomas (26). On the other hand, the inhibition of VEGF production or VEGFR phosphorylation has been shown to reduce the growth of FTC xenografts (21, 27–29).

These data suggest that the blockade of both EGFR and VEGFR kinase activities and their respective downstream targets [such as Akt and mitogen-activated protein kinase (MAPK)] can offer an attractive approach for the treatment of FTC bone metastasis. NVP-AEE788 (AEE788), a member of the 7H-pyrrolo[2,3-*d*] class of pyrimidines, is a novel, orally available dual specific tyrosine kinase inhibitor of the ErbB (EGFR) and VEGFR receptors (30). The efficacy of AEE788 against a variety of tumors (breast, lung, bladder, and squamous cell carcinoma of the oral cavity) has been verified both *in vitro* and *in vivo* (30, 31).

We hypothesized that inhibiting the phosphorylation of the EGFR and VEGFR with AEE788 in combination with paclitaxel should inhibit the growth of experimental FTC bone lesions, thus preserving the bone structure.

In the present study, we determined whether EGFR, VEGFR, and two of their downstream signaling targets, Akt and MAPK, are overexpressed in FTC. We evaluated the effects of AEE788, given alone or with paclitaxel, on the phosphorylation of these kinases, leading to cell growth arrest and apoptosis *in vitro*. We also tested whether the administration of AEE788, alone or in combination with paclitaxel, to nude mice harboring the human FTC cells implanted in the bone marrow of the tibia would block the EGFR and VEGFR signaling pathways and inhibit the progressive growth and bone lysis.

Materials and Methods

Cell lines and culture conditions. To study the biology of bone metastasis in FTC, we used the well-established human FTC cell line WRO (32). To assess the levels of the EGFR family of receptors in human thyroid cancer, we used the following cell lines: ARO, DRO, K18, K4, C643, Hth74 (anaplastic thyroid carcinoma), and NPA187 (papillary thyroid cancer). All cell lines were maintained as monolayer cultures in DMEM supplemented with 10% fetal bovine serum (FBS), nonessential amino acids, sodium pyruvate, L-glutamine, a 2-fold vitamin, and penicillin-streptomycin (all from Life Technologies, Inc., Grand Island, NY). Cell cultures were maintained and incubated as described previously (33).

Reagents. AEE788 (30), PKI166 (33), and PTK787 (28) were synthesized and generously provided by Novartis Pharma AG (Basel, Switzerland). For use *in vitro*, all three compounds were dissolved in DMSO (Sigma-Aldrich Corp., St. Louis, MO) to a concentration of 20 mmol/L and further diluted to an appropriate final concentration in DMEM. DMSO in the final solution did not exceed 0.1% (v/v). For oral administration, AEE788 was dissolved in 90% polyethylene glycol 300 plus 10% 1-methyl-2-pyrrolidinone to a concentration of 6.25 mg/mL and given to mice at a concentration of 50 mg/kg thrice weekly (30). The AEE788 solution was prepared just before being given to mice. Paclitaxel (Mead Johnson, Princeton, NJ) was diluted in HBSS to a final concentration of 1 mg/mL and given i.p. at 200 μg once weekly, a dosing regimen that was chosen based on results of previous studies at our institution (34).

For immunohistochemistry and Western blot analysis, the following antibodies were used: polyclonal rabbit anti-EGF, anti-VEGF, anti-EGFR, anti-VEGFR2, and anti–activated EGFR (Santa Cruz Biotechnology, Santa Cruz, CA); anti-HER1 (Neomarkers, Fremont, CA); anti–activated VEGFR2 (Oncogene, Cambridge, MA); monoclonal rabbit anti–activated Akt and mouse anti–activated MAPK (Cell Signaling, Beverly, MA); rabbit Akt and mouse MAPK (Cell Signaling); rat anti-mouse CD31/platelet/endothelial cell adhesion molecule-1 (PECAM-1) and rat anti-mouse CD31 peroxidase-conjugated rat anti-mouse IgG (PharMingen, San Diego, CA); mouse anti–proliferating cell nuclear antigen (anti-PCNA) clone PC-10 (DAKO A/S, Copenhagen, Denmark); peroxidase-conjugated $F(ab')_2$ goat anti-rabbit IgG $F(ab')_2$, peroxidase-conjugated rat anti-mouse IgG $F(ab')_2$ fragment, Affinipure Fab fragment goat anti-mouse IgG, peroxidase-conjugated goat anti-rat IgG, and Texas red–conjugated goat anti-rat IgG (Jackson Research Laboratories, West Grove, CA); peroxidase-conjugated rat anti-mouse IgG2a (Serotec; Harlan Bioproducts for Science, Inc., Indianapolis, IN); Alexa Fluor 594–conjugated goat anti-mouse IgG, Alexa Fluor 594–conjugated goat anti-rabbit IgG, and Alexa Fluor 488–conjugated goat anti-rabbit IgG (Molecular Probes, Eugene, OR); horseradish peroxidase–conjugated donkey anti-rabbit IgG (Amersham, Buckinghamshire, United Kingdom); and sheep anti-mouse and human IgG (Sigma-Aldrich). Other reagents were Hoechst dye 3342 (molecular weight, 615.9; Hoechst, Warrington, PA), stable 3,3′-diaminobenzidine (Research Genetics, Huntsville, AL), 3-amino-9-ethylcarbazole (BioGenex Laboratories, San Ramon, CA), and Gill's hematoxylin (Sigma-Aldrich). Prolong solution was purchased from Molecular Probes and pepsin was from Biomeda (Foster City, CA).

Propidium iodide (PI) and 3-(4,5-dimethylthiazol-2-yl)-2,5-diphenyltetrazolium bromide (MTT) were both purchased from Sigma-Aldrich. Stock solutions were prepared by dissolving 1 mg of each compound in 1 mL PBS and filtering the solution to remove particles. The solution was protected from light, stored at 4°C, and used within 1 month.

Measurement of cell proliferation. The antiproliferative activity of AEE788 on WRO cells growing in culture was determined using the tetrazolium-based colorimetric (MTT) assay. Specifically, 4×10^3 cells were plated for 24 hours into a 96-well plate. Cells were washed twice using 2% FBS medium and incubated for 72 hours with AEE788. The cells were then incubated for 2 hours in medium containing MTT and then lysed in DMSO. The conversion of MTT to formazan by metabolically viable cells was monitored by a 96-well microtiter plate reader at an absorbance of 570 nm (Dynatech, Inc., Chantilly, VA).

Measurement of cell death. The WRO cells were plated at a density of 3×10^5 cells per well in six-well plates (Costar, Cambridge, MA) and maintained in 10% FBS medium overnight. The next day, the cells were washed twice and maintained in 2% FBS medium before treatment with AEE788 and paclitaxel. Seventy-two hours later, PI staining of hypodiploid DNA was used to determine the extent of cell death. The treated cells were resuspended in Nicoletti buffer [50 mg/mL PI, 0.1% sodium citrate, 0.1% Triton X-100, and 1 mg/mL RNase A (Roche, Basel, Switzerland)] in PBS for 20 minutes at 4°C. Later, cells were analyzed by flow cytometry, and the sub-G_0/G_1 fraction was measured using the Lysis program (Becton Dickinson, Franklin Lakes, NJ). The percentage of cells undergoing specific apoptosis was calculated by subtracting the percentage of cells that had undergone spontaneous apoptosis in the relevant controls from the total percentage of apoptotic cells in the study cultures.

Western blot analysis of phosphorylated epidermal growth factor receptor/epidermal growth factor receptor, phosphorylated vascular endothelial growth factor receptor 2/vascular endothelial growth factor receptor, phosphorylated Akt/Akt, and phosphorylated mitogen-activated protein kinase/mitogen-activated protein kinase in follicular thyroid carcinoma. The ability of AEE788 to inhibit EGF-induced tyrosine phosphorylation of EGFR, VEGFR, MAPK, and Akt was determined in the human WRO FTC cell line. Under serum-free conditions, the WRO cells showed a low level of autophosphorylation that was enhanced after exposure to recombinant human EGF for 15 minutes. Cells were plated onto a six-well plate at a concentration of 4×10^5 cells per well and incubated in 10% FBS medium overnight. The next day, the cells were washed and incubated with serum-free medium for 24 hours. The study wells were treated with AEE788 at a concentration of 0.01 to 5 μmol/L, whereas the control wells were treated with DMSO for 1 hour. Then, cells were activated with recombinant human EGF (40 ng/mL) for 15 minutes, washed with PBS, and scraped with lysis buffer as described previously (31). The proteins (70 μg) were resolved on 10% SDS-PAGE and transferred onto

0.45 mmol/L polyvinylidene difluoride membranes. The membranes were probed overnight with the desired primary antibodies. After incubation with appropriate secondary antibodies, signals were visualized by the Super-Signal West Pico Chemiluminescent system from Pierce (Rockford, IL).

PCR analysis of epidermal growth factor receptor mutations. To determine whether the WRO cell line harbors EGFR mutations that might render it more sensitive to AEE788, PCR analysis was used to amplify exons 18, 19, and 21 from the human *EGFR* gene by using genomic DNA isolated from the WRO cell line. The sequences of PCR primers are the same as the ones reported previously (35). PCR amplicons were purified using QIAquick PCR purification kit (Qiagen, Valencia, CA) and sent for sequencing. The sequencing results were then blasted and compared with the wild-type *EGFR* sequence from Genbank.

Injection of WRO cells into the tibia of nude mice. Male athymic nude mice were purchased from the animal production area of the National Cancer Institute-Frederick Cancer Research Facility (Frederick, MD) and maintained in specific pathogen-free barrier animal facilities approved by the American Association for Accreditation of Laboratory Animal Care. They were used for experiments at ages 8 to 12 weeks. To produce bone tumors, WRO cells were harvested from subconfluent cultures by a 2-minute exposure to 0.25% trypsin and 0.02% EDTA. Trypsinization was stopped with medium containing 10% FBS, and the cells were washed once in serum-free medium and resuspended in Ca^{2+}- and Mg^{2+}-free HBSS. Nude mice were anesthetized with i.p. sodium pentobarbital (commonly known as Nembutal; Abbott Laboratories, North Chicago, IL) at a 50 mg/kg concentration. A percutaneous intraosteal injection was made by drilling a 27-gauge needle into the tibia immediately proximal to the tuberositas tibiae. After penetration of the cortical bone, the needle was inserted into the shaft of the tibia, and 20 μL of the cell suspension (4×10^5 cells) were deposited in the bone cortex using a calibrated, pushbutton-controlled dispensing device (Hamilton Syringe Co., Reno, NV). To prevent leakage of cells into the surrounding muscles, a cotton swab was held for 1 minute over the site of injection. The animals tolerated the surgical procedure well, and no anesthesia-related deaths occurred.

Therapy for human follicular thyroid carcinoma cells growing in the tibia of athymic nude mice. Three days after the intratibial injection of the WRO cells, the nude mice were randomized into four groups ($n = 13$): (*a*) the control group received oral administrations of the vehicle solution (90% polyethylene glycol 300 + 10% 1-methyl-2-pyrrolidinone) thrice weekly and a once weekly i.p. injection of HBSS; (*b*) the paclitaxel group received an i.p. injection of 200 μg paclitaxel once weekly; (*c*) the AEE788 group received oral administrations of 50 mg/kg AEE788 thrice weekly; and (*d*) the AEE788 plus paclitaxel group received 50 mg/kg AEE788 orally thrice weekly and a once weekly i.p. injection of 200 μg paclitaxel. The mice were treated for 5 weeks.

Digital radiography, tumor harvest, and tissue preparation. After 2, 3, 4, and 5 weeks of treatment, mice from all groups were anesthetized with sodium pentobarbital and placed in a prone position. Digital radiography was carried out using the Faxitron machine (Faxitron X-ray Corp., Wheeling, IL; ref. 36). Tumor incidence and size were recorded. The mice were euthanized by carbon dioxide inhalation on week 5 of the study (after 4 weeks of treatment) and weighed. Both legs were resected at the head of the femur and weighed. The net tumor weight was calculated by subtracting the weight of the uninjected leg from that of the leg with a tumor. The presence of a tumor in bone was confirmed by histologic examination. Tumor tissues were cut into 2 to 3 mm^3 pieces that included the tibia and surrounding muscles. The fragments were fixed in 10% buffered formalin for 24 hours at room temperature, washed with PBS for 30 minutes, decalcified with 10% EDTA (pH 7.4) for 7 to 10 days at 4°C, and then embedded in paraffin. The method described by Mori et al. (37) was used for the preparation of frozen sections with the following modifications: tumors cut into 2 to 3 mm^3 pieces were fixed in periodate-lysine-paraformaldehyde solution (4% paraformaldehyde containing 0.075 mol/L lysine and 0.01 mol/L sodium periodate) for 24 hours, washed with PBS for 30 minutes, decalcified with 10% EDTA (pH 7.4) for 7 to 10 days, and washed thrice (once with PBS containing 10% sucrose for 4 hours, once with PBS containing 15% sucrose for 4 hours, and once with PBS containing 20% sucrose for 16 hours). All procedures were carried out at 4°C. The tissues were then embedded in OCT compound (Miles, Inc., Elkhart, IN), frozen rapidly in liquid nitrogen, and stored at −80°C.

Immunohistochemical-immunofluorescent determination of epidermal growth factor, vascular endothelial growth factor, epidermal growth factor receptor, activated epidermal growth factor receptor, vascular endothelial growth factor receptor, activated vascular endothelial growth factor receptor, Akt, activated Akt, mitogen-activated protein kinase, activated mitogen-activated protein kinase, proliferating cell nuclear antigen, terminal deoxynucleotidyl transferase–mediated dUTP nick end labeling, and CD31/platelet/endothelial cell adhesion molecule-1. To examine the activity of AEE788, tumor specimens were processed for routine histologic and immunohistochemical analyses for markers of vascularization, survival, proliferation, and cell death. *In vivo* cell proliferation and apoptosis were evaluated using anti-PCNA antibodies and terminal deoxynucleotidyl transferase–mediated dUTP nick end labeling (TUNEL), respectively. Paraffin-embedded tissues were used for identification of PCNA, EGF, VEGF, EGFR, and VEGFR2. The sections were dried overnight, deparaffinized in xylene, and dehydrated in a graded series of alcohol followed by rehydration in PBS. Sections analyzed for PCNA and VEGFR2 were microwaved for 5 minutes for antigen retrieval, whereas sections analyzed for VEGF and EGFR were incubated for 20 minutes with pepsin at 37°C for antigen retrieval as described previously. Frozen tissues were used for identification of CD31/PECAM-1, activated EGFR, activated VEGFR2, activated MAPK, activated Akt, and TUNEL. The tissues were sectioned mounted and air dried for 30 minutes. Frozen sections were fixed in cold acetone (5 minutes), 1:1 acetone/chloroform (v/v; 5 minutes), and acetone (5 minutes) and washed with PBS. Immunohistochemical procedures were done as described previously (34). Control samples exposed to the secondary antibody alone showed no specific staining.

Immunofluorescent double staining for CD31/activated epidermal growth factor receptor, CD31/activated vascular endothelial growth factor receptor 2, and CD31/terminal deoxynucleotidyl transferase–mediated dUTP nick end labeling. To study the proposed antiangiogenic effect of AEE788 and its potential ability to inhibit EGFR and VEGFR phosphorylation on tumor-associated endothelial cells, periodate-lysine-paraformaldehyde–fixed frozen tissues were sectioned and prepared as mentioned above. Double staining (CD31/TUNEL, CD31/activated EGFR, and CD31/activated VEGFR2) was done as follows: EGFR immunostaining was done after CD31 staining. Samples were incubated with a protein-blocking solution for 5 minutes with a 1:50 dilution of rabbit polyclonal antihuman EGFR antibody (mouse cross-reactive) for 18 hours at 4°C. Secondary goat anti-rabbit antibody conjugated to FITC was added for 1 hour. The samples were with Vectashield (Vector Laboratories, Burlingame, CA). TUNEL assay was done using an apoptosis detection kit (Promega, Madison, WI).

Immunofluorescence microscopy was done in a Nikon Microphot-FX (Nikon, Inc., Garden City, NY) equipped with a HBO 100 mercury lamp and narrow band-pass filters to individually select for green, red, and blue fluorescence (Chroma Technology Corp., Brattleboro, VT). Images were captured using a cooled charged coupled device Hamamatsu 5810 camera (Hamamatsu Corp., Bridgewater, NJ) and Optimas Image Analysis software (Media Cybernetics, Silver Spring, MD). Stained sections were examined in a Nikon Microphot-FX microscope equipped with a three-chip charged coupled device color video camera (model DXC990, Sony Corp., Tokyo, Japan). Photomontages were prepared using Photoshop software (Adobe Systems, Inc., San Jose, CA). Endothelial cells were identified by red fluorescence staining, and DNA fragmentation was detected by localized green and yellow fluorescence within the nuclei of apoptotic cells. Photomontages were printed in a Sony digital color printer (model UP-D7000).

Quantification of microvessel density, terminal deoxynucleotidyl transferase–mediated dUTP nick end labeling, proliferating cell nuclear antigen, epidermal growth factor, vascular endothelial growth factor, epidermal growth factor receptor, and vascular endothelial growth factor receptor. For the quantification analysis, five slides were

prepared for each group, and two areas were selected in each slide. The percentage of stained cells among the total number of cells in each area and the average proportion of stained cells in each group were calculated and compared. For total TUNEL and PCNA expression, the positive cells were counted at ×100 magnification and divided by total number of tumor cells in 10 random 0.159-mm^2 fields adjacent to bone. The PCNA$^+$ cells were counted in the randomly selected pure tumor area and the percentage is reported as PCNA$^+$ cells divided PCNA$^+$ cells with the total number of tumor cells. Quantification of apoptotic endothelial cells was expressed as an average of the ratio of apoptotic endothelial cells to the total number of endothelial cells in 10 random 0.011-mm^2 fields at ×400 magnification. To quantify MVD, 10 random 0.159-mm^2 fields adjacent to the bone at ×100 magnification were captured for each tumor, and the mean number of vessels was quantified as described previously (38).

For the quantification of immunohistochemical intensity, the absorbance of 100 EGF$^+$, VEGF$^+$, EGFR$^+$, and VEGFR$^+$ cells in 10 random 0.039-mm^2 fields at ×200 magnification was taken from treated tumor tissues and was measured using the Optimas Image Analysis software. The samples were not counterstained so that the absorbance would be attributable solely to the product of the immunohistochemical reaction. Immunoreactivity was evaluated by computer-assisted image analysis and expressed as a density value.

Statistical analysis. Descriptive statistics including means and SDs were done. The Wilcoxon rank sum test was used to assess the effect of treatment on tumor weight and other continuous measurements (CD31/PECAM-1, CD31/TUNEL, TUNEL, and PCNA). Frequency tables were obtained by cross-classifying the treatment group and the categorical outcome. The incidence of bone lysis between different groups of mice was compared using the Fisher's exact test. All computations were carried out on a Dell personal computer using SAS software (SAS Institute, Inc., Cary, NC) and Excel 2000 (Microsoft, Redmond, WA) in a Windows NT operating system.

Results

High expression of epidermal growth factor receptor in thyroid carcinoma cells. Although anaplastic thyroid cancer constitutes only 1% of all thyroid tumors (3), it is among the most aggressive and fatal of all neoplasms. Western blotting was used to assess the level of all four members (HER1, HER2, HER3, and HER4) of the EGFR family of receptors in a panel of thyroid cancer cell lines. HER1, the most studied member of the EGFR family of receptors and commonly called EGFR, was highly expressed in the WRO cell line by comparison with the papillary thyroid cancer NPA187 cell line and most of the anaplastic thyroid cancer cell lines (Fig. 1*A*). Moreover, the WRO cells had the highest expression of HER2 and HER4 receptors (Fig. 1*A*). No expression of HER3 was detected in any of the thyroid cancer cell lines studied (data not shown).

AEE788 inhibits the epidermal growth factor–induced phosphorylation of epidermal growth factor receptor, vascular endothelial growth factor receptor 2, Akt, and mitogen-activated protein kinase in follicular thyroid carcinoma cells growing in culture. Next, we determine whether AEE788 can inhibit the EGF-mediated growth and survival signaling pathways in FTC growing in culture. WRO cells were starved of serum overnight, treated with increasing concentrations of AEE788 for 1 hour, and then stimulated with EGF for 15 minutes. Western blots revealed that the inhibition of EGFR phosphorylation required 0.05 μmol/L, whereas complete abrogation of phosphorylated VEGFR2 phosphorylation required 5 μmol/L AEE788 (Fig. 1*B*). The phosphorylated forms of both Akt and MAPK were down-modulated in cells treated with 0.5 μmol/L AEE788. Total levels of EGFR, VEGFR, Akt, and MAPK remained unaltered by AEE788 treatment (Fig. 1*B*).

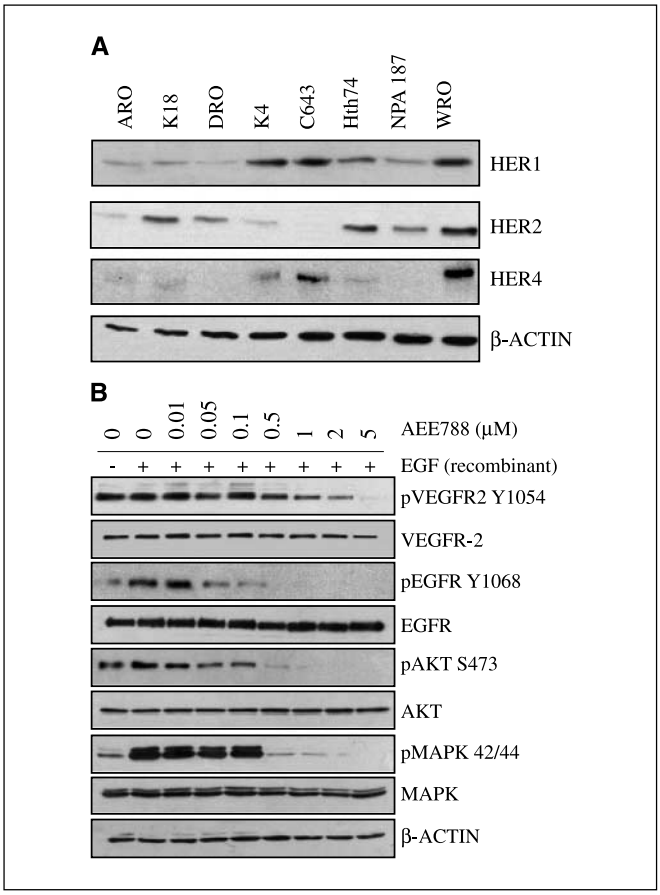

Figure 1. Expression of EGFR family members in thyroid cancer cell lines and dose-dependent inhibition of EGFR and VEGFR signaling in WRO FTC cells after treatment with AEE788. *A*, Western blotting was used to assess the level of expression of the EGFR family of receptors in thyroid cancer cell lines. Blots were additionally probed with anti-β-actin antibody for equal loading. Representative of three independent experiments. *B*, autophosphorylation of EGFR, VEGFR2, MAPK, and Akt was evaluated in WRO cells growing *in vitro* in serum-free medium and stimulated with recombinant human EGF (40 ng/mL) for 15 minutes in the presence or absence of AEE788. Western blotting was done on protein extracts, and the membrane was later probed with anti-human EGFR phosphorylated at Tyr^{1068} (*pEGFR Y1068*), VEGFR2 phosphorylated at Tyr^{1045} (*pVEGFR2 Y1054*), MAPK phosphorylated at Thr^{42}/Thr^{44} (*pMAPK 42/44*), and Akt phosphorylated at Ser^{473} (*pAKT S473*). Total EGFR, VEGFR2, MAPK, and Akt protein levels remained constant. β-Actin protein expression was used as an internal probe for equal loading. Representative of three independent experiments.

AEE788 suppresses the *in vitro* proliferation of follicular thyroid carcinoma cells and sensitizes the cells to paclitaxel-mediated cytotoxicity. The growth of the WRO cells in medium containing 2% FBS was inhibited by AEE788 at an IC$_{50}$ of 2.65 μmol/L (Fig. 2*A*). Furthermore, WRO cells exhibited paclitaxel-mediated growth inhibition at an IC$_{50}$ of 3.78 nmol/L (Fig. 2*B*), which was amplified by the addition of 0.5 μmol/L AEE788 (i.e., lowering the IC$_{50}$ from 3.78 to 2.67 nmol/L). The AEE788-mediated increase in the sensitivity of the WRO cell line to chemotherapy, however, was evident only at the lower concentrations of paclitaxel (Fig. 2*B*). To elucidate the importance of EGFR versus VEGFR inhibition on proliferation, WRO cells were treated with either an EGFR inhibitor (PKI166), a VEGFR inhibitor (PTK787), or a combination of both (PKI166 + PTK787). Cell growth was inhibited by PKI166 and PTK787 treatment alone at an IC$_{50}$ of 4.26 and 9.12 μmol/L, respectively.

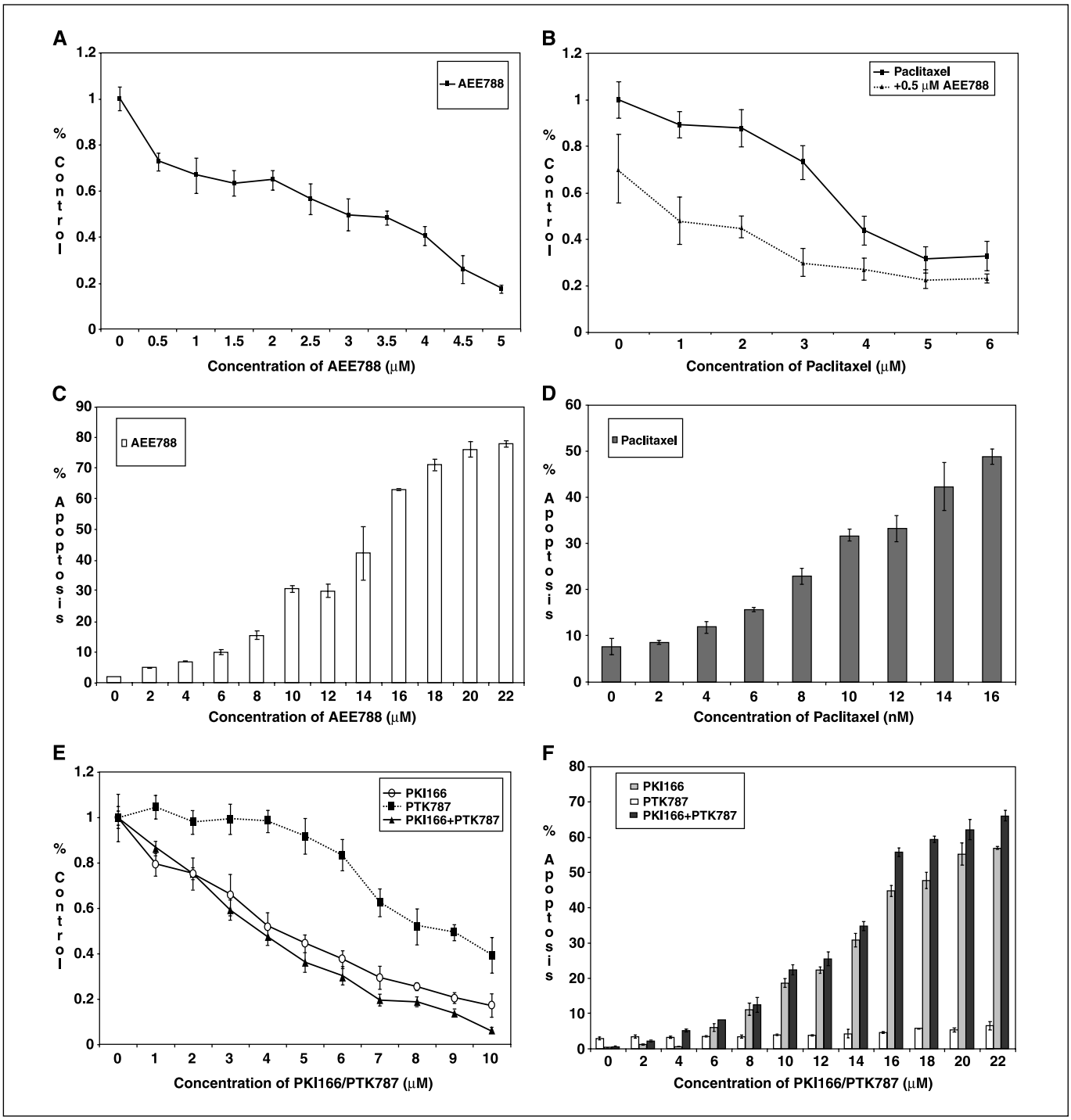

Figure 2. Antiproliferative effects of AEE788 versus PKI166/PTK787 on the WRO human FTC cell line. MTT and flow cytometry–based assays were done to determine the effects of AEE788 used alone or in combination with paclitaxel on the proliferation and apoptosis of cultured WRO FTC cells. Dose-dependent growth inhibition of (*A*) AEE788 alone, (*B*) AEE788 given with increasing doses of paclitaxel, PKI166, and PTK787 alone, or in combination (*E*). *Points*, average of at least three experiments. AEE788 also induced apoptosis (*C*) in a dose-dependent fashion with an IC_{50} of 14.7 μmol/L after 72 hours of treatment. Similarly, paclitaxel induced apoptosis (*D*) of WRO FTC cells with an IC_{50} approaching 16 nmol/L. PKI166 treatment alone induced dose-dependent cell death with an IC_{50} of 18 μmol/L, whereas PTK787 alone did not induce high levels of apoptosis even at the highest dose tested (22 μmol/L). When combined, PKI166 + PTK787 showed an IC_{50} of 15.2 μmol/L (*F*).

When both drugs were combined at equal doses, WRO cell proliferation was inhibited at an IC_{50} of 3.88 μmol/L (Fig. 2*E*).

AEE788 and paclitaxel induce apoptosis of follicular thyroid carcinoma cells *in vitro*. Next, we analyzed the ability of AEE788 and paclitaxel to induce apoptosis in WRO cells. The cells were incubated with increasing concentrations of each drug alone, and apoptosis was determined by a flow cytometry–based assay. After 72 hours of treatment with AEE788, 50% of the cells underwent apoptosis at 14.7 μmol/L. At 22 μmol/L, ~80% cell death was achieved (Fig. 2*C*). In parallel, paclitaxel induced apoptosis in the

WRO cells with an IC_{50} of 16 nmol/L (Fig. 2*D*). No sensitizing effect of AEE788 (at 2 and 4 μmol/L) on the paclitaxel-induced apoptosis of FTC cells was detected when both drugs were added simultaneously (data not shown). When compared with AEE788 alone, PKI166 plus PTK787 combination induced comparable levels of apoptosis with an IC_{50} of 15.2 μmol/L (Fig. 2*F*). PKI166 alone achieved 50% of cell death at 18 μmol/L. On the other hand, PTK787 alone failed to induce high levels of apoptosis even at the highest dose tested (22 μmol/L).

PCR analysis of epidermal growth factor receptor shows no mutations in the WRO cell line. Two recent studies have suggested that the clinical responsiveness to therapies like gefitinib—originally designed to target the phosphorylation of EGFR in human lung cancer—is closely correlated with specific mutations in exons 18, 19, and 21 of the human *EGFR* gene. Such mutations led to increased growth factor signaling and conferred susceptibility to inhibition by gefitinib (35). In light of the susceptibility of WRO to AEE788 treatment, we investigated whether such mutations also exist in this cell line. EGFR mutational analysis did not find mutations in exons 18, 19, and 21 of the *EGFR* gene in the WRO cell line (data not shown).

The follicular thyroid carcinoma cells grow progressively and induces osteoblastic and osteolytic bone lesions in nude mice. To study the biology of bone metastases secondary to FTC, we adopted the established murine model of bone lesions (15, 36, 39) by injecting the WRO cells into the tibia of athymic nude mice followed with weekly radiographic imaging. By the start of the third week, early signs of bone lesions, as evidenced by thinning of the bone, were evident (Fig. 3*A*). Bone lysis was visible by the fourth week; by the fifth week, advanced bone destruction with marked erythema of the overlying soft tissue was visible (Fig. 3*A*). This progressive bone lysis over time was detected in 80% of the injected mice. H&E staining of serial sections of the injected tibias revealed osteoblastic and osteolytic lesions (Fig. 3*B*), which are common to FTC (10).

AEE788, alone and in combination with paclitaxel, inhibits the growth of follicular thyroid carcinoma in the tibia of nude mice. To assess the effect of AEE788 on the *in vivo* growth of FTC cells in bone, the previously described mouse model was used (15, 36, 39). Digital radiography of the injected tibias revealed that 80% of the mice in the control group had progressive bone lysis. The incidence of lytic bone lesions in the mice treated with paclitaxel was not significant (Table 1). As shown in Fig. 3*C* and *D*, severe bone lysis was detected in both the control and the paclitaxel-treated groups. AEE788, as a single agent, did not decrease tumor incidence but markedly reduced the extent of bone lysis (Fig. 3*C* and *D*). AEE788 combined with paclitaxel significantly reduced the incidence of bone lysis (45%; $P < 0.05$). In the mice given oral AEE788 alone, bone integrity was maintained. The best preservation of bone structure was in mice treated with the AEE788 plus paclitaxel.

AEE788 treatment significantly reduced tumor weight compared with control and paclitaxel-treated tumors ($P < 0.05$; Table 1). The combination of paclitaxel plus AEE788 produced higher reduction in bone lesions ($P < 0.05$; Table 1).

Histologic and immunohistochemical analyses. To assess the extent of microscopic disease in the injected tibias, tumors were processed for routine histology. H&E staining revealed the presence of tumor cells within the medullary canal of the proximal tibia, the extent of bone destruction, and the extravasation of tumors into the surrounding soft tissues. The mice in the control and paclitaxel-treated groups had extensive tumors, destruction of the surrounding cortical bone, and extrusion of the WRO cells into the surrounding soft tissues (Fig. 3*D*). In contrast, most tumors in mice treated with AEE788 alone or with AEE788 plus paclitaxel were much smaller, did not destroy the cortical bone architecture, and were contained within the bone space (Fig. 3*D*).

AEE788 blocks epidermal growth factor receptor and vascular endothelial growth factor receptor signaling in follicular thyroid carcinoma cells growing in the bone. Immunohistochemical studies revealed that the level of expression of EGF, VEGF, EGFR, and VEGFR did not vary significantly among tumors from all groups (Table 2; Fig. 4*A*). Conversely, the status of EGFR and VEGFR activation differed markedly in tumors from the mice treated with AEE788 alone and AEE788 plus paclitaxel in comparison with the control and paclitaxel-treated mice. When antibodies specific to tyrosine-phosphorylated (activated) EGFR and VEGFR were used, both receptors showed high levels of phosphorylation in the absence of AEE788 treatment. High levels of phosphorylation were markedly reduced in tumors treated with AEE788 alone and AEE788 plus paclitaxel (Fig. 4*B*).

The status of two of the major downstream targets of EGFR and VEGFR pathways, Akt and MAPK, was also assessed by immunohistochemical analysis. No change in the level of expression of total Akt and MAPK proteins was evident in the four groups (Fig. 5*A*). However, the phosphorylation status of both kinases, although high in the control and paclitaxel-treated tumors, was distinctly down-regulated in the mice treated with AEE788 alone and AEE788 plus paclitaxel (Fig. 5*A*).

AEE788 arrests cell proliferation and induces apoptosis in follicular thyroid carcinoma cells growing in bone. In addition to the inhibition of EGFR and VEGFR signaling, the decrease in tumor weight in mice treated with AEE788 and AEE788 plus paclitaxel could have been due to a reduction in tumor cell proliferation, increased tumor cell apoptosis, or a combination of both.

To examine *in vivo* cell proliferation and apoptosis, antibodies were used against PCNA and the TUNEL assay, respectively. As shown in Fig. 4*B*, $PCNA^+$ cells were mostly abundant in the control group and decreased in the treated tumors. In addition, $TUNEL^+$ cells were rarely detected in tumors from the control mice. A progressive increase in the green fluorescent apoptotic cells was found in the tumors from the treated mice.

The percentage of detected $PCNA^+$ cells was significantly reduced in the AEE788-treated groups, and the percentage was lowest in the AEE788 plus paclitaxel group ($P < 0.05$; Table 2). The percentage of dying cells in mice treated with AEE788 or AEE788 plus paclitaxel was significantly higher than in the control group ($P = 0.034$; Table 2).

AEE788 suppresses angiogenesis by inhibiting epidermal growth factor receptor and vascular endothelial growth factor receptor phosphorylation and inducing apoptosis in tumor-associated endothelial cells. When antibodies were used against CD31 on the surface of endothelial cells, the MVD was highest in the control group and paclitaxel-treated tumors (Table 2). MVD was significantly ($P < 0.05$) decreased in the tumors treated with AEE788 alone and AEE788 plus paclitaxel, respectively (Table 2; Fig. 5*B*). Double staining for CD31/activated EGFR and CD31/activated VEGFR—done with CD31 (red staining) and activated EGFR and activated VEGFR (green staining)—revealed that only tumors from the mice treated with AEE788 and AEE788 plus paclitaxel had decreased double staining (yellow color) for these markers, a finding consistent with reduced

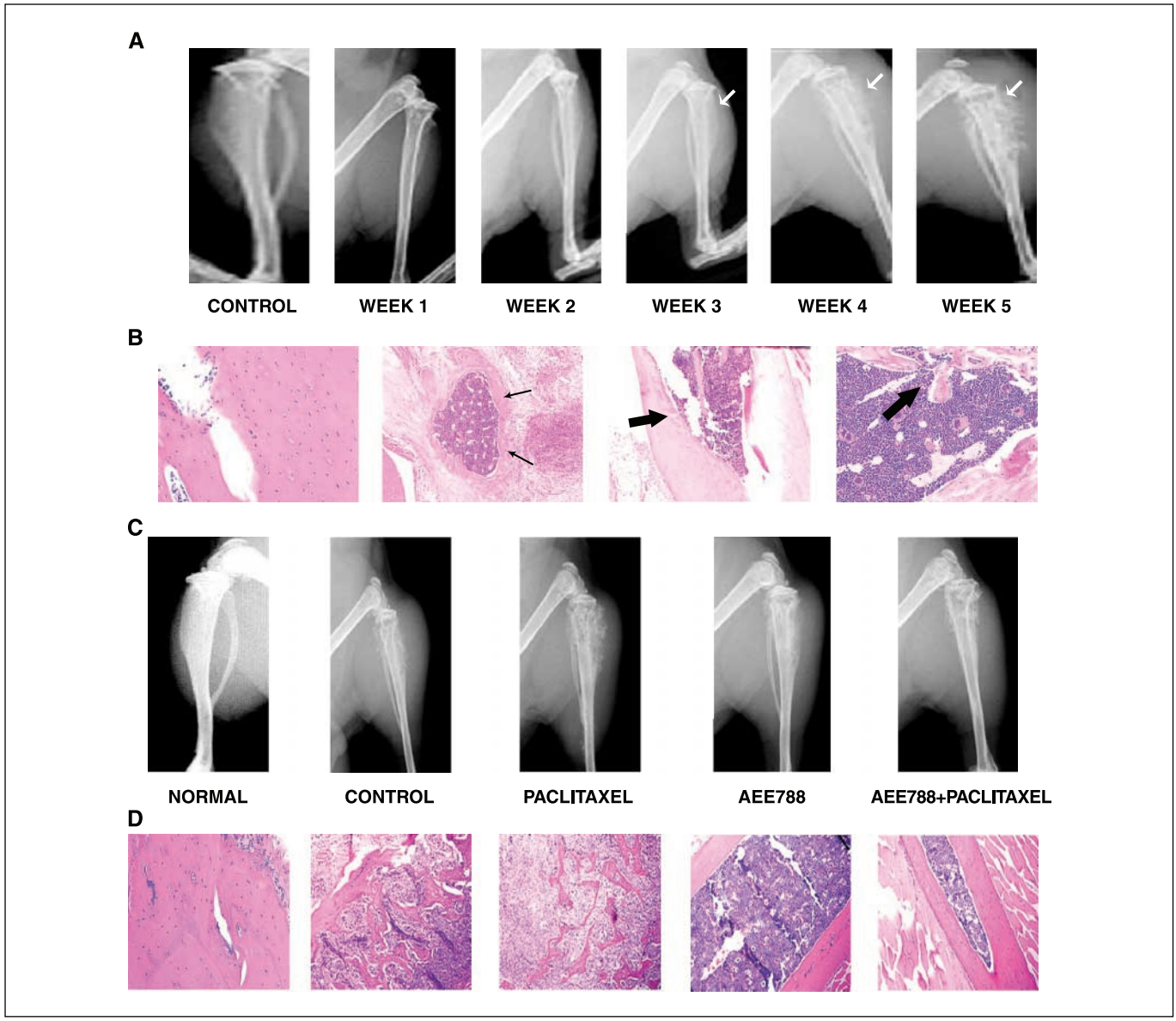

Figure 3. Effect of AEE788 on bone lesions secondary to FTC in a model for bone metastasis in nude mice. *A*, WRO cells were injected into the right tibia of athymic nude mice. Bone lysis was detected (*white arrows*) as early as the third week and progressed to severe cortical bone destruction by the end of 5 weeks. *B*, H&E staining of bone tumors after the fifth week. Note the osteoblastic lesions (*thin black arrows*) and osteolytic lesions (*thick black arrows*) in comparison with normal bone (*right*). *C* and *D*, mice were segregated into four treatment groups. The mice in the control group and those treated with paclitaxel had large tumors with extensions into the surrounding tissue. AEE788 alone or in combination with paclitaxel preserved the integrity of the cortical bone and maintained the tumor cells within the bony space as seen by H&E staining.

signaling through EGFR and VEGFR in endothelial cells (Fig. 5*B*). Finally, double staining for CD31 (red staining)/TUNEL (green staining) showed that the percentage of apoptotic endothelial cells (yellow staining) was significantly higher in the bone tumors of mice treated with AEE788 alone and AEE788 plus paclitaxel than in the control and those treated with paclitaxel alone ($P < 0.05$; Table 2; Fig. 5*B*).

Discussion

In our study, AEE788 and paclitaxel effectively inhibited cellular proliferation and induced apoptosis of FTC growing in culture. In addition, AEE788 suppressed the phosphorylation of EGFR, VEGFR, Akt, and MAPK in FTC. In a mouse model for bone lesions, WRO cells grew progressively and produced mainly osteolytic and some osteoblastic lesions. The oral administration of AEE788 alone, thrice weekly or in combination with once weekly i.p. injections of paclitaxel, significantly reduced the incidence and size of bone lesions and prevented bone lysis as determined by digital radiography and confirmed by histologic examination. Immunohistochemical analyses showed the *in vivo* inhibition of activated EGFR and VEGFR signaling pathways and downstream Akt and MAPK activities in WRO-induced bone lesions from mice treated with AEE788 alone or in combination with paclitaxel. Consequently, tumor cell proliferation ($PCNA^+$ cells) was suppressed, and tumor cell apoptosis ($TUNEL^+$ cells)

Table 1. Results of treatment with AEE788 and paclitaxel for human FTC growing in the bones of nude mice

Treatment groups*	Lytic lesion incidence (%)†	Tumor weight (g), median (range)
Control	8/10 (80)	0.29 (0.074-0.547)
Paclitaxel	8/9 (89)	0.375 (0.175-2.484)
AEE788	7/8 (88)	0.118‡ (0.011-0.253)
AEE788 + paclitaxel	5/11 (45)	0.048‡ (0.004-1.377)

*WRO human FTC cells (4×10^5) were injected into the tibia of nude mice. Three days later, groups of mice were randomized into four groups: i.p. injections of paclitaxel (200 μg) alone (once weekly), oral feedings of AEE788 (500 mg/kg) alone (thrice weekly), paclitaxel in combination with AEE788, or placebo (control). All mice were killed after 5 weeks of treatment.

† Number of mice with lytic lesions visualized by digital radiography divided by the number of mice injected.

‡ $P < 0.05$, compared with controls (Wilcoxon rank sum test).

was induced. In addition, AEE788 alone and in combination with paclitaxel silenced the EGFR and VEGFR signaling on the surface of tumor-associated endothelial cells. In response, endothelial cells ($TUNEL^+/CD31^+$ cells) underwent apoptosis, leading to a significant reduction in MVD.

In vitro, AEE788 alone showed enhanced growth inhibition of WRO cells compared with PKI166 plus PTK787 combination. This may be attributed to the fact that AEE788, in addition to its primary inhibition of EGFR and VEGFR pathways, can also inhibit c-Src, c-kit, and RET pathways at higher doses (30). All three pathways have been shown to play a pivotal role in the tumorigenesis of thyroid carcinomas (40). PTK787 treatment alone did not induce high levels of apoptosis and high doses of PTK787 were needed to induce cell growth inhibition. This suggests that the effect of AEE788, at least *in vitro*, is mainly attributable to inhibition of EGFR. Although inhibition of the VEGFR is seen in tumor cells *in vitro*, this does not seem to have an effect on tumor cell survival or proliferation, as does inhibition of the EGFR, and highlights the importance of testing this compound *in vivo* to determine the effect of VEGFR inhibition. Whereas EGFR is seen to localize to the endothelia and tumor cells, the inhibition of VEGFR kinase activity is thought to contribute to endothelial cell apoptosis and decreased MVD with resultant increase in tumor cell apoptosis.

Our present results closely agree with our previous work (41) and other studies (42) reporting that EGFR is overexpressed in differentiated and anaplastic thyroid carcinomas and that targeting EGFR by anti-EGFR antibodies (EGFR antibody 528) completely neutralized the EGF-mediated stimulation of FTC cell growth and invasion in culture (19). Furthermore, our findings agree with studies showing that genistein, a general tyrosine kinase antagonist, can abrogate growth stimulation of EGF and transforming growth factor-α (TGF-α) on invasion and growth of FTC cells (19).

At present, our data have shown that radiographically there was a significant reduction in bone destruction in mice treated with AEE788 alone or with AEE788 plus paclitaxel. One possible explanation is that TGF-α and EGF increased the proliferation of osteoclast precursors, thus inducing a surge in the number of osteoclasts leading to bone lysis. Blockade of EGFR signaling by

Table 2. Quantitative immunohistochemical analysis of WRO human FTC tumors growing in the tibia of nude mice

Variable	Treatment groups			
	Control	Paclitaxel	AEE788	AEE788 + paclitaxel
Tumor cells				
PCNA*	21.55 ± 2.95	15.12 ± 3.81	9.17 ± 1.89†	6.63 ± 2.37†
TUNEL*	6.76 ± 2.72	14.08 ± 6.5	44.12 ± 14.64†	54.89 ± 14.07†
EGF (absorbance)‡	0.94 ± 0.33	0.88 ± 0.30§	1.1 ± 0.35§	0.89 ± 0.25§
VEGF (absorbance)‡	1.23 ± 0.45	1.20 ± 0.44§	1.35 ± 0.46§	1.33 ± 0.48§
EGFR (absorbance)‡	0.31 ± 0.18	0.33 ± 0.1§	0.42 ± 0.11§	0.36 ± 0.11§
VEGFR (absorbance)‡	0.52 ± 0.17	0.6 ± 0.14§	0.55 ± 0.17§	0.69 ± 0.10§
Endothelial cells				
CD31*	12.62 ± 3.66	11 ± 3.77	5.79 ± 1.49†	6.13 ± 2.09†
CD31/TUNEL‖	1 (0-3)	2 (0-3)	12 (6-19)†	16 (9-25)†

*Mean ± SD, ratio of positive cells to total tumor/endothelial cells, as determined from measurement of 10 random 0.159-mm^2 fields at ×100 magnification.

† $P < 0.05$ (Wilcoxon rank sum test).

‡ Absorbance determined as described in Materials and Methods.

§ $P > 0.05$ (Wilcoxon rank sum test).

‖ Median of the ratio of apoptotic endothelial cells to total number of endothelial cells in 10 random 0.011-mm^2 fields at × 400 magnification.

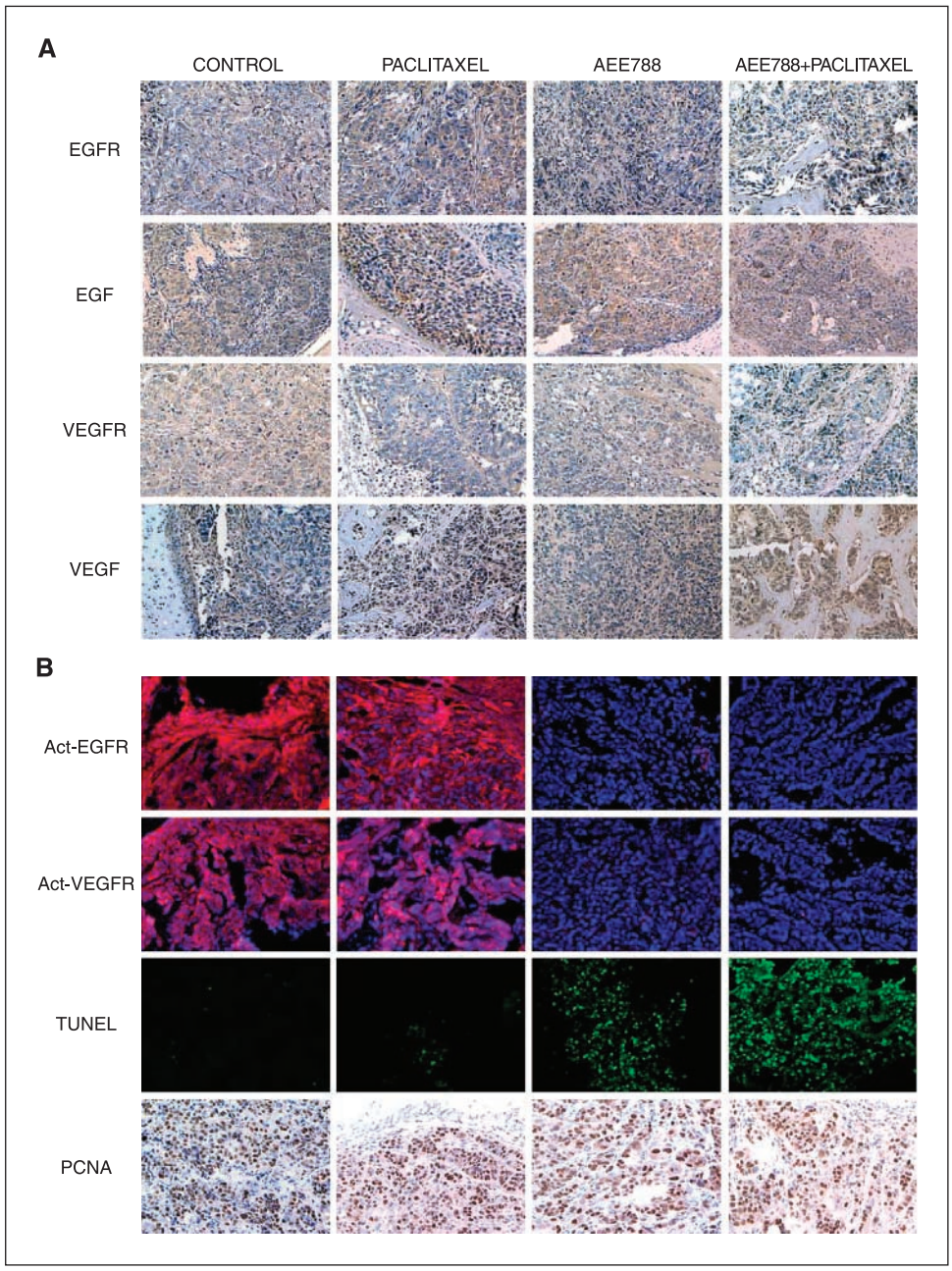

Figure 4. Dual inhibition of EGFR and VEGFR phosphorylation and increased tumor apoptosis in FTC-induced bone lesions after treatment with AEE788 alone or in combination with paclitaxel. Bone tumors of the WRO FTC cells that have been injected into the tibia of nude mice were harvested and processed for immunohistochemical analysis after the fifth week of treatment with HBSS and AEE788 vehicle (control), once weekly i.p. injection of paclitaxel (200 μg once weekly), thrice weekly oral administration of AEE788 (50 mg/kg), or a combination of both regimens. *A,* immunohistochemical analysis using specific anti-EGF, anti-VEGF, anti-EGFR, and anti-VEGFR antibodies showed that WRO tumors from all four treatment groups exhibited similar levels of EGF, VEGF, EGFR, and VEGFR. *B,* specific antibodies to phosphorylated EGFR and phosphorylated VEGFR were used to assess the activation status of these receptors. The tumors from mice treated with AEE788 alone or in combination with paclitaxel showed diminished phosphorylation of EGFR and VEGFR in comparison with tumors from nontreated (control group) and paclitaxel-treated mice. Tumors from all four groups were also stained for PCNA and TUNEL. Treatment with AEE788, with or without paclitaxel, reduced expression of PCNA (*brown staining*) and increased apoptosis as marked by TUNEL$^+$ cells (*green fluorescent staining*). Magnification, ×100.

AEE788 may therefore decrease the number and activity of osteoclasts (43).

In our study and others (44), the active phosphorylated forms of VEGFR2 receptors were not found on the endothelial cells in the uninjected leg (data not shown). Moreover, we have shown that VEGFR2 was expressed in both the FTC cells and the tumor-associated endothelial cells. VEGFR2 phosphorylation was inhibited by treatment with AEE788 treatment under *in vitro* and *in vivo* conditions. PTK787 has shown antitumoral and antiangiogenic activity against FTC xenografts (28). Furthermore, soluble VEGF receptor (*sFlt-1*) gene therapy effectively reduced the growth of FTC xenografts (27). Mice treated with an anti-VEGF antibody (monoclonal antibody 4.6.1) develop smaller FTC tumors containing few blood vessels (21). Furthermore, endostatin protein and gene therapy have proven to be effective in suppressing the growth of FTC xenografts (29). Collectively, the down-modulation of VEGF signaling can produce inhibition of differentiated thyroid cancer growth *in vivo*.

Increased vascularity has been reported in thyroid tumors (45). In thyroid cancer, increased MVD has been correlated with decreased disease-free survival (28). Similarly, MVD in the areas of the most intense vascularization is an independent prognostic factor in patients with breast and non–small cell lung cancer (46, 47). In our study, oral administration of AEE788 alone or in combination with paclitaxel significantly decreased MVD. Most endothelial cells in normal tissues and organs are quiescent and do not divide. In contrast, endothelial cells in many tumors are dividing. Proliferating endothelial cells have been shown to express low levels of EGFR (34). In our study, only the tumor-associated endothelial cells from the mice treated with AEE788 alone or in combination with paclitaxel

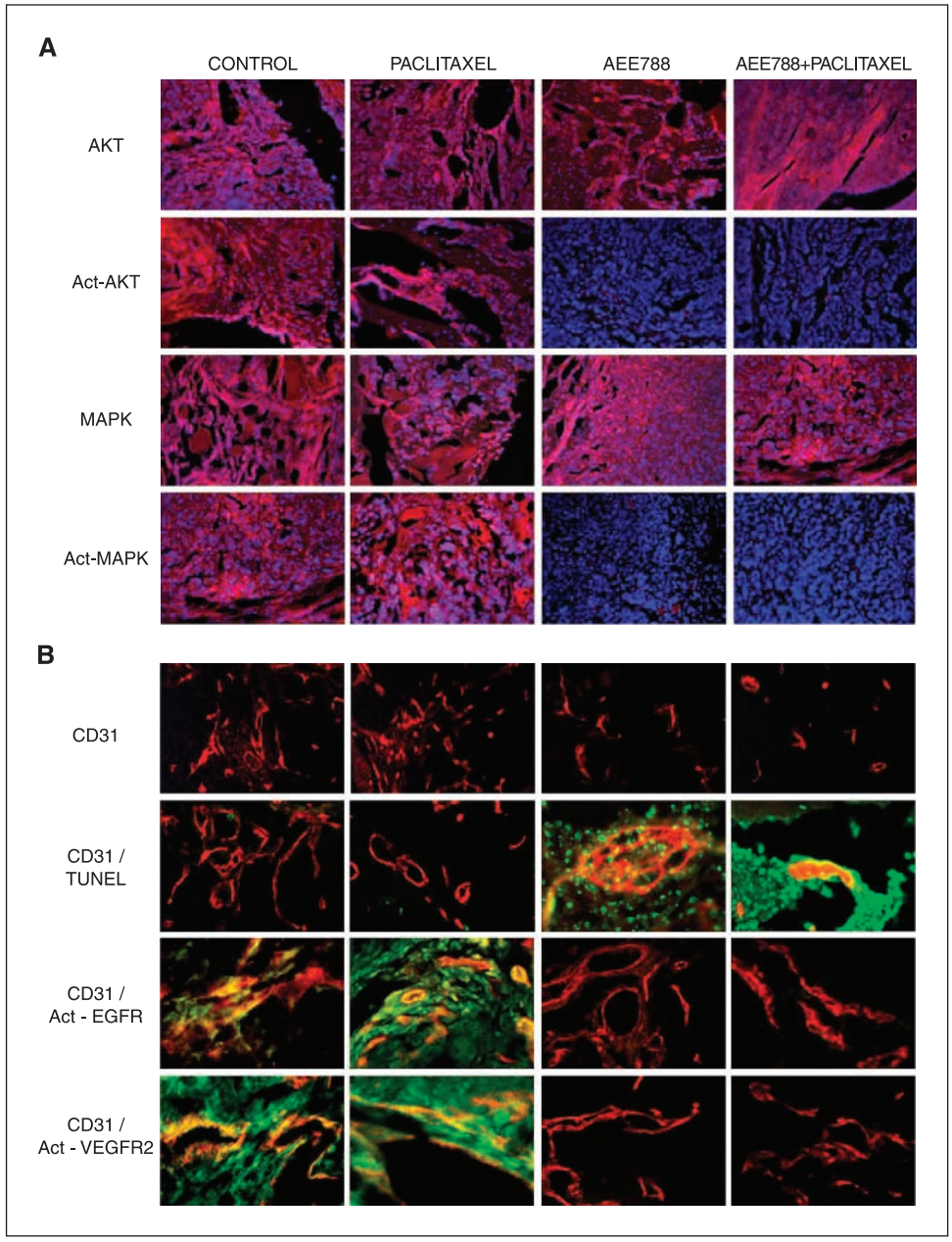

Figure 5. Inhibition of downstream kinase phosphorylation in tumors and suppression of angiogenesis as determined by reduction in MVD, inhibition of receptor phosphorylation, and induction apoptosis after treatment with AEE788. *A,* WRO tumors growing in the tibia of mice were stained for activated Akt (*Act-Akt*), total Akt, activated MAPK (*Act-MAPK*), and total MAPK. Although tumors from all four groups showed similar patterns of expression for total Akt and MAPK, tumors from mice treated with AEE788 alone or in combination with paclitaxel had a marked reduction in the level of Akt and MAPK phosphorylation compared with the control and paclitaxel-treated tumors. *B,* MVD status was assessed using antibodies against CD31/PECAM-1 (*red staining*). In mice treated with AEE788 with or without paclitaxel, CD31/PECAM-1 reduction was noted. Double staining for CD31 (*red*)/TUNEL (*green*) revealed induction of apoptosis in tumor-associated endothelial cells in both AEE788-treated tumors (*yellow staining*). Double staining for CD31/activated EGFR (*Act-EGFR*) and CD31/activated VEGFR (*Act-VEGFR2*) was done with CD31 (*red staining*) and with activated EGFR and activated VEGFR (*green staining*). Suppression of the phosphorylation of EGFR and VEGFR on the surface of endothelial cells (marked by the absence of *yellow color*) was detected only in the AEE788-treated tumors with or without paclitaxel administration. Magnification, ×400.

had reduced double staining for CD31/activated EGFR and CD31/activated VEGFR. Thus, it is possible that FTC cells stimulate EGFR activation in endothelial cells by a paracrine mechanism through the production of EGF and possibly TGF-α. The loss of major survival signals in endothelial cells might render them more susceptible to taxane-based therapy. Crippling such vital signaling pathways and inducing apoptosis in endothelial cells can create a second wave of apoptosis in the adjacent tumor cells. This is in agreement with a study in which paclitaxel was found to enhance the antitumor efficacy of DC101, a VEGFR2-blocking antibody, by potentiating the antiangiogenic response and inducing tumor and endothelial cell apoptosis (48).

Despite the significant reduction in tumor size and incidence of bone lysis in the groups of mice treated with AEE788 and paclitaxel, 55% of the animals exhibited bone lysis on digital radiography. It has been postulated that blocking the EGFR signaling pathway reduced activator protein-1 activity and hence the transcription of VEGF (34). In our study, no reduction in VEGF expression could be detected by immunohistochemical analysis in tumors from either group of mice treated with AEE788. One possible explanation for the apparent discrepancy is that VEGF expression in thyroid carcinomas is regulated by additional growth factors, including insulin-like growth factor-I (IGF-I; ref. 49). In fact, IGF-I is produced by stromal cells in the microenvironment of thyroid carcinomas (50), promotes proliferation (51), and suppresses apoptosis (52) of thyroid carcinoma cells. These observations coupled with the fact that IGF-I receptor is expressed on the surface of thyroid tumors (53) give FTC an alternative route for growth and progression.

The phosphorylation status of two major downstream targets of EGFR and VEGFR pathways, Akt and MAPK, was down-regulated in FTC tumors growing in bone after AEE788 treatment. This finding is in agreement with previous studies. Basically, the expression of all

three isoforms of Akt are expressed in FTC (54). More importantly, increased levels of phosphorylated Akt were higher in FTC than in normal thyroid tissue (55). FTC cells invading the thyroid capsule or blood vessels, or metastasizing to other areas, have been characterized by activation of Akt in a nuclear pattern, suggesting an association between Akt activity and progression of tumors (54). Our laboratory has shown that the inhibition of Akt phosphorylation by a novel Akt inhibitor successfully suppressed cellular growth and induced apoptosis in thyroid cancer cells (56).

Another important molecule that has been found to be upregulated in patients with bone metastasis from FTC is MAPK (57). The RAS-RAF-extracellular signal-regulated kinase (ERK)-MAPK/ERK kinase-MAPK pathway is of particular importance in FTC tumorigenesis because of the higher prevalence of activating mutations of all three Ras genes (58). Total MAPK was detected in equal amounts in both tumors and normal tissues of the thyroid, whereas phosphorylated MAPK was more prevalent in thyroid tumors than in adjacent normal thyroid tissue (59). U0126, a MAPK/ERK kinase-1/2 inhibitor, decreased phosphorylated MAPK and reduced the cell viability of FTC cells *in vitro* (59).

Collectively, our results provide experimental evidence that AEE788 can block bone lesions induced by FTC by inhibiting the EGFR pathway on FTC cells and inhibiting angiogenesis by suppressing the VEGFR signaling pathway in tumor-associated endothelial cells. Our present findings closely agree with our previous work that showed that dual blockade of EGFR and VEGFR signaling with AEE788 inhibits the growth of human squamous cell carcinoma of the oral cavity (31) and squamous cell carcinoma of the skin in nude mice and produces apoptosis of tumor-associated endothelial cells (60).

In summary, we show that the simultaneous blockade of EGFR and VEGFR signaling by AEE788 alone or in combination with paclitaxel can significantly reduce tumor size and subsequent bone destruction by FTC in the bone of nude mice mediated by both direct antitumor and antiangiogenic effects. These data strongly recommend further development of AEE788 for clinical use in the treatment of FTC patients with bone metastases.

Acknowledgments

Received 11/23/2004; revised 3/9/2005; accepted 3/31/2005.

Grant support: Golfers against Cancer and The University of Texas M.D. Anderson Cancer Center Specialized Programs of Research Excellence in Head and Neck Cancer grant P50 CA97007.

The costs of publication of this article were defrayed in part by the payment of page charges. This article must therefore be hereby marked *advertisement* in accordance with 18 U.S.C. Section 1734 solely to indicate this fact.

We thank Sandy Young for editorial review and Patricia A. Phillips for expert assistance in the submission of the article.

References

1. Correa P, Chen VW. Endocrine gland cancer. Cancer 1995;75:338–52.
2. Jemal A, Tiwari RC, Murray T, et al. Cancer statistics, 2004. CA Cancer J Clin 2004;54:8–29.
3. Sherman SI. Thyroid carcinoma. Lancet 2003;361:501–11.
4. Hundahl SA, Cady B, Cunningham MP, et al. Initial results from a prospective cohort study of 5583 cases of thyroid carcinoma treated in the United States during 1996. U.S. and German Thyroid Cancer Study Group. An American College of Surgeons Commission on Cancer Patient Care Evaluation Study. Cancer 2000; 89:202–17.
5. Lin JD, Huang MJ, Juang JH, et al. Factors related to the survival of papillary and follicular thyroid carcinoma patients with distant metastases. Thyroid 1999;9: 1227–35.
6. Schlumberger MJ. Papillary and follicular thyroid carcinoma. N Engl J Med 1998;338:297–306.
7. Schlumberger M, Tubiana M, De Vathaire F, et al. Long-term results of treatment of 283 patients with lung and bone metastases from differentiated thyroid carcinoma. J Clin Endocrinol Metab 1986;63:960–7.
8. DeGroot LJ, Kaplan EL, Shukla MS, Salti G, Straus FH. Morbidity and mortality in follicular thyroid cancer. J Clin Endocrinol Metab 1995;80:2946–53.
9. Marcocci C, Pacini F, Elisei R, et al. Clinical and biologic behavior of bone metastases from differentiated thyroid carcinoma. Surgery 1989;106:960–6.
10. Roodman GD. Mechanisms of bone metastasis. N Engl J Med 2004;350:1655–64.
11. Tubiana M, Haddad E, Schlumberger M, Hill C, Rougier P, Sarrazin D. External radiotherapy in thyroid cancers. Cancer 1985;55:2062–71.
12. Smit JW, Vielvoye GJ, Goslings BM. Embolization for vertebral metastases of follicular thyroid carcinoma. J Clin Endocrinol Metab 2000;85:989–94.
13. Menzel C, Grunwald F, Schomburg A, et al. "High-dose" radioiodine therapy in advanced differentiated thyroid carcinoma. J Nucl Med 1996;37:1496–503.
14. Dinneen SF, Valimaki MJ, Bergstralh EJ, et al. Distant metastases in papillary thyroid carcinoma: 100 cases observed at one institution during 5 decades. J Clin Endocrinol Metab 1995;80:2041–5.
15. Weber KL, Doucet M, Price JE, Baker C, Kim SJ, Fidler IJ. Blockade of epidermal growth factor receptor signaling leads to inhibition of renal cell carcinoma growth in the bone of nude mice. Cancer Res 2003;63: 2940–7.
16. Tuttle M, Robbins R, Larson SM, Strauss HW. Challenging cases in thyroid cancer: a multidisciplinary approach. Eur J Nucl Med Mol Imaging 2004;31: 605–12.
17. Zettinig G, Fueger BJ, Passler C, et al. Long-term follow-up of patients with bone metastases from differentiated thyroid carcinoma-surgery or conventional therapy? Clin Endocrinol (Oxf) 2002; 56:377–82.
18. Aasland R, Akslen LA, Varhaug JE, Lillehaug JR. Co-expression of the genes encoding transforming growth factor-α and its receptor in papillary carcinomas of the thyroid. Int J Cancer 1990;46:382–7.
19. Holting T, Siperstein AE, Clark OH, Duh QY. Epidermal growth factor (EGF)- and transforming growth factor α-stimulated invasion and growth of follicular thyroid cancer cells can be blocked by antagonism to the EGF receptor and tyrosine kinase *in vitro*. Eur J Endocrinol 1995;132:229–35.
20. Gorgoulis V, Aninos D, Priftis C, et al. Expression of epidermal growth factor, transforming growth factor-α and epidermal growth factor receptor in thyroid tumors. *In vivo* 1992;6:291–6.
21. Soh EY, Eigelberger MS, Kim KJ, et al. Neutralizing vascular endothelial growth factor activity inhibits thyroid cancer growth *in vivo*. Surgery 2000;128: 1059–65;discussion 1065–56.
22. Hanahan D, Folkman J. Patterns and emerging mechanisms of the angiogenic switch during tumorigenesis. Cell 1996;86:353–64.
23. Soh EY, Duh QY, Sobhi SA, et al. Vascular endothelial growth factor expression is higher in differentiated thyroid cancer than in normal or benign thyroid. J Clin Endocrinol Metab 1997;82:3741–7.
24. Bunone G, Vigneri P, Mariani L, et al. Expression of angiogenesis stimulators and inhibitors in human thyroid tumors and correlation with clinical pathological features. Am J Pathol 1999;155:1967–76.
25. Tuttle RM, Fleisher M, Francis GL, Robbins RJ. Serum vascular endothelial growth factor levels are elevated in metastatic differentiated thyroid cancer but not increased by short-term TSH stimulation. J Clin Endocrinol Metab 2002;87:1737–42.
26. Ishiwata T, Iino Y, Takei H, Oyama T, Morishita Y. Tumor angiogenesis as an independent prognostic indicator in human papillary thyroid carcinoma. Oncol Rep 1998;5:1343–8.
27. Ye C, Feng C, Wang S, et al. sFlt-1 gene therapy of follicular thyroid carcinoma. Endocrinology 2004;145: 817–22.
28. Schoenberger J, Grimm D, Kossmehl P, Infanger M, Kurth E, Eilles C. Effects of PTK787/ZK222584, a tyrosine kinase inhibitor, on the growth of a poorly differentiated thyroid carcinoma: an animal study. Endocrinology 2004;145:1031–8.
29. Ye C, Feng C, Wang S, Liu X, Lin Y, Li M. Antiangiogenic and antitumor effects of endostatin on follicular thyroid carcinoma. Endocrinology 2002;143: 3522–8.
30. Traxler P, Allegrini PR, Brandt R, et al. AEE788: a dual family epidermal growth factor receptor/ErbB2 and vascular endothelial growth factor receptor tyrosine kinase inhibitor with antitumor and antiangiogenic activity. Cancer Res 2004;64:4931–41.
31. Yigitbasi OG, Younes MN, Doan DD, et al. Tumor and endothelial cell therapy of oral cancer by dual tyrosine receptor blockade. Cancer Res 2004;64:7977–84.
32. Estour B, Van Herle AJ, Juillard GJ, et al. Characterization of a human follicular thyroid carcinoma cell line (UCLA RO 82 W-1). Virchows Arch B Cell Pathol Incl Mol Pathol 1989;57:167–74.
33. Holsinger FC, Doan DD, Jasser SA, et al. Epidermal growth factor receptor blockade potentiates apoptosis mediated by paclitaxel and leads to prolonged survival in a murine model of oral cancer. Clin Cancer Res 2003;9:3183–9.
34. Bruns CJ, Solorzano CC, Harbison MT, et al. Blockade of the epidermal growth factor receptor signaling by a novel tyrosine kinase inhibitor leads to apoptosis of endothelial cells and therapy of human pancreatic carcinoma. Cancer Res 2000;60:2926–35.
35. Lynch TJ, Bell DW, Sordella R, et al. Activating mutations in the epidermal growth factor receptor underlying responsiveness of non-small-cell lung cancer to gefitinib. N Engl J Med 2004;350:2129–39.

36. Kim SJ, Uehara H, Yazici S, et al. Simultaneous blockade of platelet-derived growth factor-receptor and epidermal growth factor-receptor signaling and systemic administration of paclitaxel as therapy for human prostate cancer metastasis in bone of nude mice. Cancer Res 2004;64:4201–8.

37. Mori S, Sawai T, Teshima T, Kyogoku M. A new decalcifying technique for immunohistochemical studies of calcified tissue, especially applicable to cell surface marker demonstration. J Histochem Cytochem 1988;36:111–4.

38. Baker CH, Solorzano CC, Fidler IJ. Blockade of vascular endothelial growth factor receptor and epidermal growth factor receptor signaling for therapy of metastatic human pancreatic cancer. Cancer Res 2002; 62:1996–2003.

39. Uehara H, Kim SJ, Karashima T, et al. Effects of blocking platelet-derived growth factor-receptor signaling in a mouse model of experimental prostate cancer bone metastases. J Natl Cancer Inst 2003;95:458–70.

40. Inaba M, Umemura S, Satoh H, et al. Expression of RET in follicular cell-derived tumors of the thyroid gland: prevalence and implication of morphological type. Pathol Int 2003;53:146–53.

41. Schiff B, McMurphy A, Jasser S, et al. Epidermal growth factor receptor (EGF-R) is overexpressed in anaplastic thyroid cancer, and the EGF-R inhibitor gefitinib ("Iressa," ZD 1839) inhibits the growth of anaplastic thyroid cancer. Clin Cancer Res 2004;10: 8594–602.

42. Bergstrom JD, Westermark B, Heldin NE. Epidermal growth factor receptor signaling activates met in human anaplastic thyroid carcinoma cells. Exp Cell Res 2000;259:293–9.

43. Roodman GD. Biology of osteoclast activation in cancer. J Clin Oncol 2001;19:3562–71.

44. Kim SJ, Uehara H, Karashima T, Shepherd DL, Killion JJ, Fidler IJ. Blockade of epidermal growth factor receptor signaling in tumor cells and tumor-associated endothelial cells for therapy of androgen-independent human prostate cancer growing in the bone of nude mice. Clin Cancer Res 2003;9:1200–10.

45. Ramsden JD. Angiogenesis in the thyroid gland. J Endocrinol 2000;166:475–80.

46. Weidner N, Semple JP, Welch WR, Folkman J. Tumor angiogenesis and metastasis-correlation in invasive breast carcinoma. N Engl J Med 1991;324:1–8.

47. Fontanini G, Lucchi M, Vignati S, et al. Angiogenesis as a prognostic indicator of survival in non-small-cell lung carcinoma: a prospective study. J Natl Cancer Inst 1997;89:881–6.

48. Inoue K, Slaton JW, Perrotte P, et al. Paclitaxel enhances the effects of the anti-epidermal growth factor receptor monoclonal antibody ImClone C225 in mice with metastatic human bladder transitional cell carcinoma. Clin Cancer Res 2000;6:4874–84.

49. Poulaki V, Mitsiades CS, McMullan C, et al. Regulation of vascular endothelial growth factor expression by insulin-like growth factor I in thyroid carcinomas. J Clin Endocrinol Metab 2003;88:5392–8.

50. Vella V, Sciacca L, Pandini G, et al. The IGF system in thyroid cancer: new concepts. Mol Pathol 2001;54: 121–4.

51. Saito J, Kohn AD, Roth RA, et al. Regulation of FRTL-5 thyroid cell growth by phosphatidylinositol (OH) 3 kinase-dependent Akt-mediated signaling. Thyroid 2001;11:339–51.

52. Mitsiades CS, Poulaki V, Mitsiades N. Insulin-like growth factor (IGF)-1 protects thyroid carcinoma cells from TRAIL-induced apoptosis. Proc Am Assoc Cancer Res 2001;42:272.

53. Yashiro T, Ohba Y, Murakami H, et al. Expression of insulin-like growth factor receptors in primary human thyroid neoplasms. Acta Endocrinol (Copenh) 1989;121: 112–20.

54. Vasko V, Saji M, Hardy E, et al. Akt activation and localisation correlate with tumour invasion and oncogene expression in thyroid cancer. J Med Genet 2004;41: 161–70.

55. Ringel MD, Hayre N, Saito J, et al. Overexpression and overactivation of Akt in thyroid carcinoma. Cancer Res 2001;61:6105–11.

56. Mandal M, Younes MN, Jasser SA, El-Naggar AK, Mills GB, Myers JN. The Akt inhibitor KP372-1 suppresses Akt activity and cell proliferation and induces apoptosis in thyroid cancer cells. Br J Cancer. In press 2005.

57. Chen KT, Lin JD, Chao TC, et al. Identifying differentially expressed genes associated with metastasis of follicular thyroid cancer by cDNA expression array. Thyroid 2001;11:41–6.

58. Lemoine NR, Mayall ES, Wyllie FS, et al. High frequency of ras oncogene activation in all stages of human thyroid tumorigenesis. Oncogene 1989;4: 159–64.

59. Specht MC, Barden CB, Fahey TJ III. p44/p42-MAP kinase expression in papillary thyroid carcinomas. Surgery 2001;130:936–40.

60. Park YW, Younes MN, Jasser SA, et al. AEE788, a dual tyrosine kinase inhibitor of EGFR and VEGFR, induces endothelial cell apoptosis in human cutaneous squamous cell carcinoma xenografts in nude mice. Clin Cancer Res 2005;11:1963–73.